J|A|C|S
COMMUNICATIONS

Ammonia Borane Confined by a Metal−Organic Framework for Chemical Hydrogen Storage: Enhancing Kinetics and Eliminating Ammonia

Zhongyue Li,[†,‡] Guangshan Zhu,[†] Gaoqing Lu,[‡] Shilun Qiu,*[,†] and Xiangdong Yao*[,‡,§]

State Key Laboratory of Inorganic Synthesis and Preparative Chemistry, College of Chemistry, Jilin University, Changchun 130012, China, ARC Centre of Excellence for Functional Nanomaterials, The University of Queensland, St Lucia, Queensland 4072, Australia, and Queensland Micro- and Nanotechnology Centre, Griffith University, Nathan, Queensland 4111, Australia

Received December 7, 2009; E-mail: sqiu@jlu.edu.cn; x.yao@griffith.edu.au

In the past few years, much attention has been focused on ammonia borane (AB), NH_3BH_3, which is considered to be a promising candidate as a hydrogen storage material[1] to meet the 2010 targets (6 wt % and 45 g L^{-1}) and potentially meet the 2015 targets (9 wt % and 81 g L^{-1}) set by the U.S. Department of Energy (DOE).[2] AB merits this attention because of its extremely high stoichiometric hydrogen content (19.6 wt %), moderate decomposition temperature, and stability at room temperature.[3] Although DOE addresses irreversibility by off-board regeneration, which releases a critical barrier for such materials for practical applications, there are still some technical challenges that must be achieved: (1) reducing the dehydrogenation temperature of AB (<85 °C set by DOE); (2) significantly increasing the hydrogen release rate; and (3) preventing the formation of volatile byproducts (e.g., borazine, ammonia, and diborane). Recently, several strategies have been developed to increase the hydrogen release rate at a relatively low temperature, such as nanoscaffolds,[4] metallic catalysis,[5] ionic liquids,[6] metal (Li,[7] Ca,[8] etc.) and methane[9] substitution, Ir[10] or Ru[11] complex catalysis, and extremely high pressure treatment.[12] The hydrogen release kinetics has been significantly increased, as reported in these references. However, the improvement is not big enough to satisfy the DOE targets for recharging time. More importantly, the literature contains no reports of the prevention of ammonia formation during AB decomposition. The elimination of ammonia is the most important issue because a very small amount of ammonia (ppm level) poisons the catalysts of proton exchange membrane (PEM) fuel cells, which are the expected application of AB for hydrogen storage.

Our recent research[13] indicated that there is a synergistic effect of combining nanoconfinement and a metallic catalyst (Li^+) on the enhancement of the hydrogen release kinetics and prevention of ammonia formation. It was proposed that the metallic catalyst is likely to interact with the $-NH_3$ group in AB, which would strengthen the N−B bond. This would contribute to the prevention of NH_3 formation. The nanoconfined system should control the particle size of AB precisely. It was also hypothesized that a stronger nanoconfinement effect should be obtained with smaller pore sizes of the host materials. Accordingly, metal−organic frameworks (MOFs) with metallic sites and micropores could be ideal frameworks to test the hypothesis: metal sites can prevent the formation of ammonia, and small pores (<1 nm) can contribute strong nanoconfinement. MOFs are a kind of porous material constructed by metal centers and organic ligands through self-assembly.[14] Their pore shapes and sizes and metal centers can be designed and controlled through the selection of different metal centers and organic ligands.[15]

Herein we report the successful synthesis of a MOF-confined AB system (denoted as AB/JUC-32-Y) by the infusion method. JUC-32-Y was selected as the framework because of its proper microporous size, high surface area, and high thermal stability and the fact that it contains open unsaturated metal sites.[16] JUC-32-Y is constructed with the rare-earth metal Y^{3+} and the rigid organic ligand 1,3,5- benzenetricarboxylate (BTC) through coordination bonding. It has a three-dimensional (3D) permanent porous skeleton that is stable up to 525 °C. After the terminal-coordinated H_2O molecules are removed by heating at 300 °C for 4 h, the original framework is retained. The open structure with one-dimensional (1D) tubular channels with a size of ∼6 Å is obtained. The diameter of these channels is a little bigger than the AB molecule, which should lead to a strong interaction with AB and produce smaller and more scattered AB nanoparticles. More importantly, because of the removal of the terminal-coordinated H_2O molecules, the coordination number of the Y^{3+} ions goes from 7 to 6, leading to an unsaturated metal site that may interact with AB (Figure 1d,e).

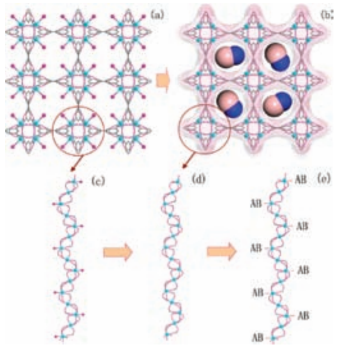

Figure 1. 3D structure image views of the (001) faces of (a) JUC-32-Y and (b) AB/JUC-32-Y. Views of 1D chains along [001] direction of JUC-32-Y (c) before and (d) after removal of terminal H_2O and (e) after interaction with AB. Y, bright blue; C, gray; O, pink; N, blue; B, purple.

AB was loaded into JUC-32-Y by infusion. The AB/JUC-32-Y molar ratio was 1:1. AB was resolved in anhydrous methanol solvent (0.5 M) at room temperature in a glovebox. The solution was inserted into the pores of JUC-32-Y by the capillary effect. The solvent was removed via vacuum at 25 °C for 24 h. The structure of JUC-32-Y remained unchanged after AB loading and after AB decomposition from the AB/JUC-32-Y, as demonstrated by the X-ray diffraction (XRD) pattern (Figure S1 in the Supporting Information). The XRD pattern of AB/JUC-32-Y did not show any peaks of AB, indicating that the AB particles were very fine and

---

[†] Jilin University.
[‡] The University of Queensland.
[§] Griffith University.

10.1021/ja9103217

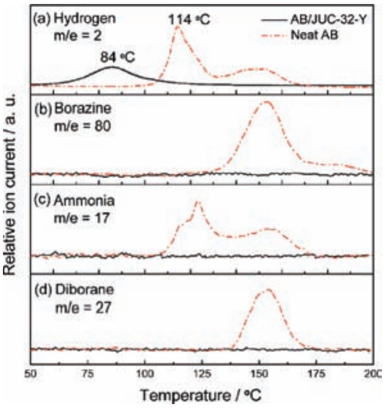

Figure 2. TPD-MS spectra of AB/JUC-32-Y (black solid line) and neat AB (red dashed line).

well-distributed. N_2 adsorption/desorption analysis (Figure S2) showed that AB/JUC-32-Y had much a smaller pore volume (0.01 $cm^3\ g^{-1}$) and BET surface area (1 $m^2\ g^{-1}$) than those of JUC-32-Y (0.27 $cm^3\ g^{-1}$ and 659 $m^2\ g^{-1}$). This demonstrated that the pores of JUC-32-Y are almost blocked with AB. Fourier transform infrared (FTIR) spectroscopy (Figure S3) exhibited some new bands at 3305, 3256, 1156, and 1067 cm^{-1}, attributable to the H−N antisymmetric stretch, H−N symmetric stretch, H−B scissor and H wag modes, respectively,[17] after AB was loaded into JUC-32-Y. All of these characterization confirmed that AB was inserted into the pores of JUC-32-Y through the capillary effect.

The AB decomposition behavior was investigated using thermogravimetric analysis (TGA), temperature-programmed desorption mass spectrometry (TPD-MS), and a pressure−composition−temperature (PCT) rig (Suzuki Shokan). Figure S4 shows that neat AB has a two-step decomposition near its melting point (112 °C) and at ∼150 °C, which is well-documented in the literature.[18] Neat AB decomposition produced a large amount of hydrogen, mixed with the unexpected byproducts borazine, ammonia, and diborane. In contrast, as shown in Figure 2, the decomposition of AB inside JUC-32-Y started at only ∼50 °C. The peak temperature of AB decomposition was shifted to 84 °C (compared with 114 °C for neat AB). This is the first reported achievement of such a big decrease (30 °C) in the decomposition temperature, confirming our hypothesis on the effect of nanoconfinement. Furthermore, no volatile products were found during the decomposition process. It should be emphasized that no ammonia was formed (Figure 2c), demonstrating our hypothesis on the prevention of ammonia formation by the metallic catalyst. The unsaturated coordination of Y^{3+} played this important role. This strongly suggested that some metals (not only Li) can be selected for this purpose. Figure 3 shows the remarkable increase in the hydrogen release rate of AB inside JUC-32-Y, which is very important for on-board applications. At 95 °C, AB inside JUC-32-Y could release 8.5 wt % hydrogen in only 3 min and reached 10.2 wt % hydrogen in only 10 min. At even a low temperature of 85 °C, AB could release 8.0 wt % hydrogen within 10 min. Neat AB does not release any hydrogen at this temperature. The Figure 3 inset also illustrates that AB confined in JUC-32-Y could release all of its theoretical hydrogen (∼13 wt % for the two-step decomposition) at 95 °C and 11 wt % of its hydrogen at 85 °C within 3 h.

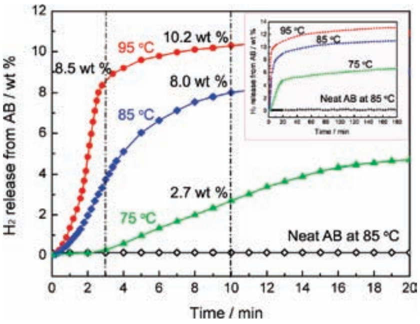

Figure 3. Time dependences of hydrogen release from AB/JUC-32-Y at 95 °C (red ●), 85 °C (blue ◆), 75 °C (green ▲) and neat AB at 85 °C (black ◇).

To date, this is the first example of the use of an MOF as the host material to improve the thermal hydrogen release of AB. Our research has confirmed the hypothesis of a synergistic effect of nanoconfinement and metallic catalysis. The small pore size of the MOF strongly confined AB, enabling decomposition at a much lower temperature. The catalytic unsaturated metal Y^{3+} sites of JUC-32-Y interacted with AB to completely prevent the formation of ammonia. The dramatic improvement of the hydrogen release kinetics, the lower operational temperature, and the high purity of the released hydrogen renders AB/MOF a very promising candidate for hydrogen storage in PEM fuel cells.

Acknowledgment. Financial support from the Australian Research Council (ARC) and the State Basic Research Project (2006CB806100) and "111" Program of the Ministry of Education in China is appreciated.

Supporting Information Available: Synthetic methods and XRD, FTIR, TGA, and N_2 adsorption/desorption data. This material is available free of charge via the Internet at http://pubs.acs.org.

References

(1) Stephens, F. H.; Pons, V.; Baker, R. T. *Dalton Trans.* **2007**, 2613.
(2) Satyapal, S.; Read, C.; Ordaz, G.; Thomas, G. *2006 Annual DOE Hydrogen Program Merit Review: Hydrogen Storage*; U.S. Department of Energy: Washington, D.C., 2006; available at:http://www.hydrogen.energy.gov/pdfs/review06/2_storage_satyapal.pdf.
(3) Karkamkar, A.; Aardahl, C.; Autrey, T. *Mater. Matters* **2007**, *2* (2), 6; available at: http://www.sigmaaldrich.com/materials-science/learning-center/material-matters.html.
(4) Gutowska, A.; Li, L.; Shin, Y. S.; Wang, C. M.; Li, X. H. S.; Linehan, J. C.; Smith, R. S.; Kay, B. D.; Schmid, B.; Shaw, W.; Gutowski, M.; Autrey, T. *Angew. Chem., Int. Ed.* **2005**, *44*, 3578.
(5) Clark, T. J.; Russell, C. A.; Manners, I. *J. Am. Chem. Soc.* **2006**, *128*, 9582.
(6) Bluhm, M. E.; Bradley, M. G.; Butterick, R.; Kusari, U.; Sneddon, L. G. *J. Am. Chem. Soc.* **2006**, *128*, 7748.
(7) Xiong, Z. T.; Yong, C. K.; Wu, G. T.; Chen, P.; Shaw, W.; Karkamkar, A.; Autrey, T.; Jones, M. O.; Johnson, S. R.; Edwards, P. P.; David, W. I. F. *Nat. Mater.* **2008**, *7*, 138.
(8) Diyabalanage, H. V. K.; Shrestha, R. P.; Semelsberger, T. A.; Scott, B. L.; Bowden, M. E.; Davis, B. L.; Burrell, A. K. *Angew. Chem., Int. Ed.* **2007**, *46*, 8995.
(9) Chen, Y. S.; Fulton, J. L.; Linehan, J. C.; Autrey, T. *J. Am. Chem. Soc.* **2005**, *127*, 3254.
(10) Denney, M. C.; Pons, V.; Hebden, T. J.; Heinekey, D. M.; Goldberg, K. I. *J. Am. Chem. Soc.* **2006**, *128*, 12048.
(11) Blaquiere, N.; Diallo-Garcia, S.; Gorelsky, S. I.; Black, D. A.; Fagnou, K. *J. Am. Chem. Soc.* **2008**, *130*, 14034.
(12) Lin, Y.; Mao, W. L.; Mao, H. K. *Proc. Natl. Acad. Sci. U.S.A.* **2009**, *106*, 8113.
(13) Li, L.; Yao, X. D.; Sun, C. H.; Du, A.; Cheng, L. N.; Zhu, Z. H.; Yu, C. Z.; Zou, J.; Smith, S. C.; Wang, P.; Cheng, H. M.; Frost, R. L.; Lu, G. Q. *Adv. Funct. Mater.* **2009**, *19*, 265.
(14) Férey, G. *Chem. Soc. Rev.* **2008**, *37*, 191.
(15) Yaghi, O. M.; O'Keeffe, M.; Ockwig, N. W.; Chae, H. K.; Eddaoudi, M.; Kim, J. *Nature* **2003**, *423*, 705.
(16) Guo, X. D.; Zhu, G. S.; Li, Z. Y.; Sun, F. X.; Yang, Z. H.; Qiu, S. L. *Chem. Commun.* **2006**, 3172.
(17) Lee, S. M.; Kang, X. D.; Wang, P.; Cheng, H. M.; Lee, Y. H. *ChemPhysChem* **2009**, *10*, 1825.
(18) Hu, M. G.; Geanangel, R. A.; Wendlandt, W. W. *Thermochim. Acta* **1978**, *23*, 249.

JA9103217